

IFSCC 2025 full paper (IFSCC2025-1093)

## ***"Efficacy and Safety of a Functional Repair Product Containing Multi-effect Repair Materials after 1565 nm Non-ablative Fractional Laser for Facial Rejuvenation in Asia"***

**Yumei Zheng<sup>1</sup>, Lina Wang<sup>1</sup>, Caixia Wang<sup>1</sup>, Yuxuan Wu<sup>1</sup>, Peiwen Sun<sup>1</sup>, Yanan Li<sup>1#</sup>, Jing Wang<sup>1\*</sup>**

<sup>1</sup>Research & Innovation Center, Proya Cosmetics Co., Ltd., Hangzhou, China

#Corresponding author: Yanan Li, e-mail: liyanan@proya.com

\* Presenting Author: Jing Wang, e-mail: wangjing48@proya.com

---

### **1. Introduction**

The rising prevalence of nonsurgical cosmetic procedures has intensified the need for effective post-treatment skincare[1], with limited clinical data. Ablative fractional laser (AFL) has long been regarded as the "gold standard" for skin rejuvenation and anti-aging in Caucasian populations in Europe and America[2]. However, due to its poorer wound-healing capacity and higher risk of post-inflammatory hyperpigmentation (PIH) in yellow race, it is rarely used for full-face ablative rejuvenation in Asian countries[3]. The non-ablative fractional laser (NAFL) has been widely used for skin rejuvenation based on "destruction-rebuild", induce collagen remodeling to improve rhytides and skin texture[4-6]. The treatment has limited effectiveness and often requires repeated treatment. Meanwhile, NAFL generates microthermal zones (MTZs) that compromise the dermal-epidermal junction (DEJ) and cell viability[7], triggers transient erythema, edema, dry, and PIH[8, 9], reducing patient acceptance despite its non-ablative nature. These limitations underscore the necessity for adjuvant therapies to enhance efficacy and mitigate side effects. Meanwhile, combination strategies also leveraging laser-induced microchannels for delivery active ingredient from care products[10].

Skin regeneration and repair can be likened to building a house. By directly providing builders with essential materials (e.g., structural components like collagen and ceramides), the skin can be remodeled more faster and efficiently[11]. Simultaneously, creating a favorable environment by reducing inflammatory stimuli further supports this regenerative process[12]. Ceramides, as integral components of the lipid matrix, can improve skin hydration, reduce inflammation, calm irritation, accelerate wound healing, and enhancing skin texture following cosmetic medicine[9]. Collagen XVII is a critical modulator in skin homeostasis, aging and wound repair[13]. Recombinant human collagen XVII (rhCOL17) can protect skin basement membrane integrity by enhancing keratinocytes migration, upregulating key components such as collagen IV, collagen VII, laminin 332 and integrin α6, and inhibiting protein phosphorylation in MAPK/Wnt pathways[14]. Crucially, NAFL-generated microchannels could facilitate penetration of these bioactive compounds, synergizing collagen stimulation with skin remodeling.

This study introduces a sequential protocol combining 1565 nm-NAFL with a novel repair essence containing rhCOL17 and Ceramide complexes (CERs). The rebuild effects of

rhCOL17 and CERs on barrier-related protein, immunity and collagen were evaluated by skin damage model in vitro. In a randomized split-face trial, we evaluate this regimen's capacity to reduce post-treatment irritation while improving rejuvenation outcomes. By addressing both therapeutic efficacy and downtime reduction, this approach aims to redefine standards for laser-based cosmetic interventions in populations prone to pigmentary complications.

## 2. Materials and Methods

### 2.1 In vivo test

#### 2.1.1 Participants

This prospective, randomized, split-face study was approved by SGS ethics committee. (SS-2024-103), and all participants provided informed consent and, conducted in accordance with the Declaration of Helsinki in 2024. A total of 32 participants were recruited for this study. Exact inclusion and exclusion requirements were established for all volunteers. Healthy men and women aged 18-48 years who been from China with balanced skin status on both sides of the face were eligible for inclusion, provided that they did not meet any of the exclusion criteria. The eligibility of each participant was evaluated by two board-certified dermatologists.

#### 2.1.2 1565-nm nonablative fractional laser and subsequent product treatments

All study participants underwent one treatment using a 1565-nm nonablative fractional laser (wavelength 1565nm, Energy 35-40mJ, Density 250 beam/cm<sup>2</sup>, ResurFX mode, M22; Lumenis®, Yokneam, Israel) on opposite sides of the face. For each patient, the treatments were applied by a single physician evaluator; and, all therapeutic parameters were the same for each patient. After therapy, the two sides of each participant's face were randomly assigned to receive one of the product (Proya® original repair essence or placebo, Proya Cosmetics Co., Ltd) treatments, them used original repair essence on one side of their faces and placebo on the other side twice a day for 28 days. Participants were instructed to refrain from using topical medications and other cosmetics containing the same effect, apart from the uniform sunscreen provided by research institutes, also, avoid sunlight exposure, for the duration of the study.

#### 2.1.3 Efficacy and safety evaluations

The treatment effectiveness and safety were assessed using objective and subjective methods. Images were captured at baseline, after single NAFL treatment, and 12 minutes, 1, 7, 14 and 28 days during subsequent original repair essence treatment using the consistent and standard posture of a VISIA® system (Canfield Scientific) and analyzed skin red area, spot, pore, and wrinkle using IPP®[15]. The surface evaluation of living skin (SELS) parameters smoothness (SEsm), roughness (SER), scaliness (SEsc) and wrinkles (SEw) on both cheeks were assessed using the Visioscan® VC 20plus (Courage+Khazaka electronic GmbH). The dermal thickness and collagen density were determined using a high-resolution ultrasound standard probe, and ultrasound images were recorded (Dermalab® Ultrasound). The stratum corneum hydration (SCH), trans-epidermal water loss (TEWL), skin tone (L\*, a\*, b\*, ITA.), erythema index (EI), and melanin index (MI), elasticity (R2, R5, R7) and firmness (R0, F4) were measured by a skin tester (MPA9, Courage+Khazaka electronic GmbH). Two skilled and experienced dermatologists evaluated the safety and efficacy at each follow-up compared with control side. All measurements were carried out in the room at a temperature of 20-22°C and an ambient humidity in the range of 40–60%. Before each return visit test, subjects were assessed after sitting in the room for 30 minutes.

#### 2.1.4 Statistical analysis

Statistical analyses were performed by using SPSS version 28.0 software; p < 0.05 was considered statistically significant. For the quantitative data, paired Student's t-test and Wilcoxon rank sum test were performed to analyze the differences between the groups; data

were shown as means  $\pm$  standard deviation (SD). Ranked data were analyzed by using the Wilcoxon rank sum test.

## 2.2 in vitro test

### 2.2.1 Ex vivo skin tissue processing

Ex vivo skin tissue (abdominal area) was derived from discarded skin of healthy female volunteer (39 years old) after operation. Access to biopsy material was in accordance with Chinese law and satisfied the requirements of the local Ethics Committee. The freshly obtained skin tissue was immersed in 75% ethanol for disinfection and rinsed for 30 seconds, followed by three washes with sterile PBS buffer. Afterward, the skin was cut into  $24\pm2$  mm<sup>2</sup> tissue blocks with the epidermal side facing upward and the dermal side facing downward. These blocks were placed in culture molds, which were transferred to 6-well plates. Each well was filled with 3.7 mL of culture medium and incubated at 37°C with 5% CO<sub>2</sub> (Thermo, 150I), with daily medium replacement. After 2 days of ex vivo skin tissue culture, irradiation and drug treatment commenced. The irradiation doses were set to UVA (30 J/cm<sup>2</sup>) and UVB (50 mJ/cm<sup>2</sup>), administered continuously for 4 days. Fresh medium was replaced after each irradiation session. The positive control (PC, 100µg/mL VC +7µg/mL VE) was administered via submersion, while test samples (0.05% rhCOL17) were applied topically. Following the 4-day irradiation period, the ex vivo skin tissues were cultured for an additional 3 days without irradiation, during which only drug treatments were continued.

### 2.2.2 3D Epidermal Model Processing

The study used EpiKutis® 3D epidermal models (ES240304, Guangdong BioCell Biotech) in 6-well plates with 0.9 mL EpiGrowth medium/well. Treatments: PC1 (0.9 mL dexamethasone medium), PC2 (0.9 mL WY14643 medium), Test (25 µL 1.5% CERS applied topically). Post-treatment, non-blank control (BC) groups received UVB irradiation (600 mJ/cm<sup>2</sup>) and incubated in CO<sub>2</sub> incubator (37°C, 5%CO<sub>2</sub>) for 24h.

### 2.2.3 Transmission electron microscopy (TEM) photography and Protein Immunofluorescence (IF) Detection

The models were fixed with 4% paraformaldehyde (PFA) for 24 hours, followed by TEM photography and IF assay. Fluorescent imaging was performed under a fluorescence microscope (Leica, DM2500), with subsequent image acquisition and quantitative analysis.

### 2.2.4 ELISA assay

Following incubation, EpiKutis® culture supernatants were collected in sterile centrifuge tubes and stored at -80°C for preservation. Subsequent analysis was performed strictly according to the manufacturer's protocol of the commercial ELISA kit.

### 2.2.5 Statistical analysis

Data were visualized using Origin 2019 and expressed as mean $\pm$ SD. Intergroup comparisons were analyzed by two-tailed Student's t-test. P<0.05 was considered statistically significant.

## 3. Results

### 3.1 Remediation Efficacy of CERs on Barrier Proteins and Inflammatory Factors

In the UVB damaged 3D epidermal model, by ELISA assay, compared to the negative control (NC) group, CERs significantly reduced the secretion of IL-1 $\alpha$  and PGE2 (P<0.05), indicating its efficacy in soothing skin inflammatory irritation by suppressing the production of these pro-inflammatory mediators. Withal, compared to the NC group, CERs significantly upregulated FLG, LOR, and Keratin 1 levels (P<0.01). These findings demonstrated that CERs effectively repairs skin barrier function by augmenting the expression of key structural proteins.

### 3.2 The remodeling capacity of rhCOL17 on the DEJ and structural proteins

In ex vivo skin models, following combined UVA and UVB irradiation, the NC group exhibited structural damage at the DEJ, including discontinuities, accompanied by significant reductions in key protein components: Laminin 5, collagen IV, collagen VII, collagen XVII ( $P<0.05$ ). The major structural proteins of the skin dermis, collagen I and III, were also significantly reduced ( $P<0.05$ ). Compared to the NC group, treatment with rhCOL17 resulted in improved structural continuity of the DEJ, accompanied by significantly elevated levels of Laminin 5, collagen IV, collagen VII, collagen XVII, collagen I, and collagen III (Figure 1,  $P<0.05$ ). These findings demonstrated the rhCOL17's ability to ameliorate DEJ damage and enhance the structural integrity of both the DEJ and dermal matrix. Moreover, rhCOL17 also significantly upregulated the content of barrier proteins (FLG, LOR, Keratin 10).

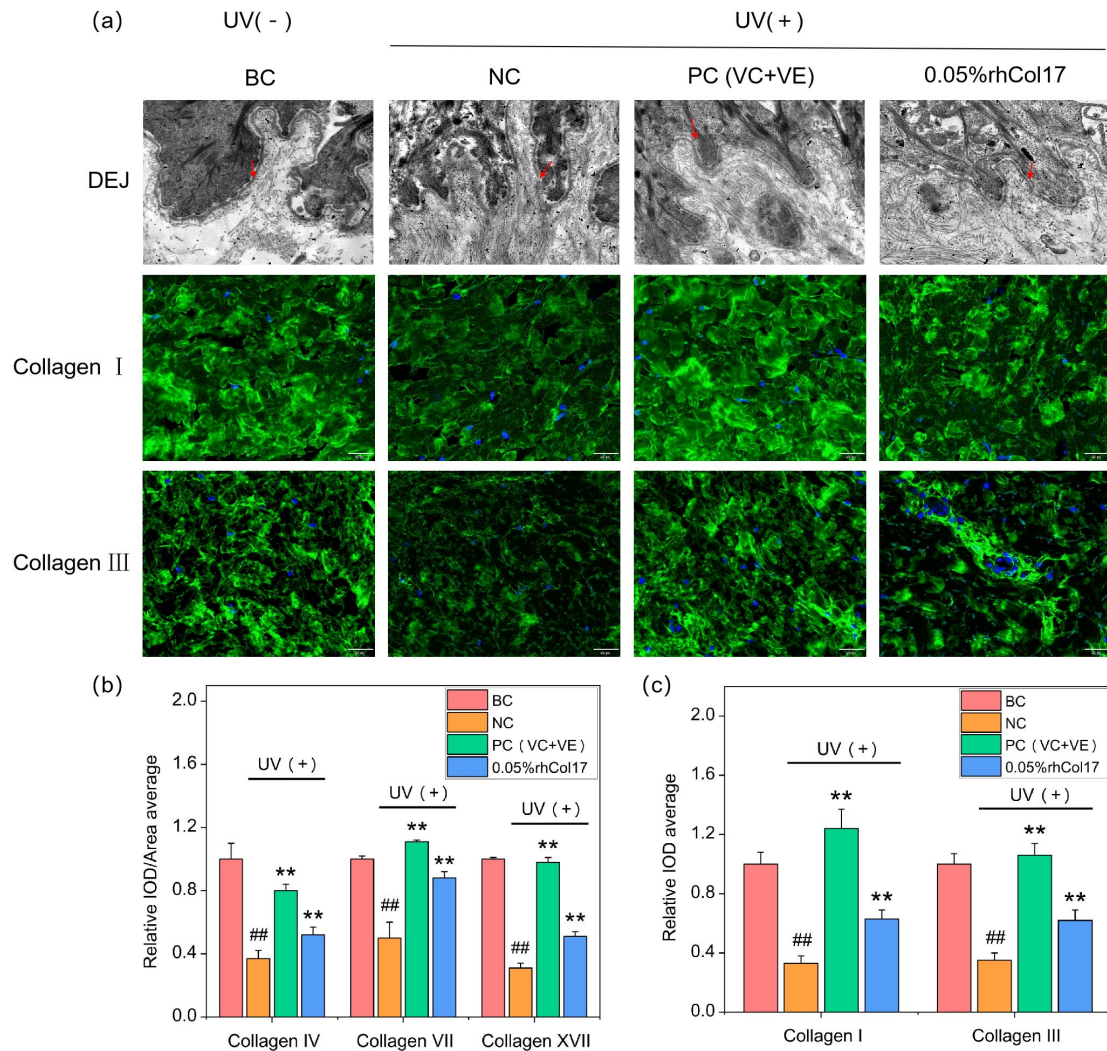


**Figure 1 The remodeling capacity of rhCOL17 on the DEJ and structural proteins.** (a) gray photos are TEM photos, taken at 60,000-fold, red arrows indicate the DEJ structure, where the NC group marks the damaged area. Collagen I and III were photographed by fluorescence microscope. Bar=50 $\mu$ m. Blue fluorescence is the nucleus, and green fluorescence is Collagen I and III, respectively. The more green fluorescence, the brighter it is, indicating the higher content of Collagen I and III. (b) Integrated optical density (IOD) /Area, which reflects Collagen IV, VII and XVII content from DEJ. (c) IOD reflects the Collagen I and III content form dermis. For statistical analysis by t-test method, compared with BC group, significance was denoted as #, P-value < 0.01 was denoted as ##; Compared with NC group, significance is expressed as \*, P-value < 0.01 as \*\*.

3.3 Efficacy and Safety of the sequential protocol combining 1565 nm-NAFL with a novel repair essence containing rhCOL17 and CERs for facial rejuvenation  
3.3.1 General information of the subjects

The participants were 5 men and 27 women with Fitzpatrick skin types ranged from II to V in this clinical study, and the mean age was  $33.8 \pm 8.4$  years (range, 20-48 years). All completed NAFL treatment, as well as followup visits at 12 minutes, 1, 7, 14 and 28 days during subsequent original repair essence treatment. Before using the product, the skin redness, fine line, and spot pigmentation score on either side before treatment and after single NAFL treatment did not differ significantly.

### 3.3.2 Dermatologist's subjective safety assessment

After single NAFL treatment, the main irritation symptoms of edema and erythema (100% incidence) persisted for about 24 hours or so and gradually disappeared, in which erythema lasted longer, and erythema and edema observed by the naked eye could disappear within a week. The erythema of the skin was relieved with the repair essence applied immediately after the laser, which was statistically different from that on the control side. However, the effect on edema was not significant, and more than 30% of the subjects' edema symptoms resolved by the second day after the laser, while the erythema took longer to resolve. Other adverse effects including pruritus sensation (22% incidence), thermal sensation (91% incidence), burning sensation (97% incidence), tightness sensation (97% incidence), tingling sensation (97% incidence), and drying/desquamation (100% incidence) were observed only at the visit of the point of immediate follow-up time after NAFL treatment on either side. Immediate use of product relieved and disappeared thermal, burning, tightness, tingling sensation, and drying/desquamation after NAFL treatment, the difference between the two sides was statistically significant.

### 3.3.3 Objective assessments

The use of instruments to test the skin is often more accurate to capture more subtle changes. Therefore, objective instrumental measurements of skin redness, hydration, TEWL, topography, color, wrinkles, elasticity, and collagen density, before and after the NAFL were performed.

#### (1) Skin sensitivity and barrier function

Skin red colour response can be used as an indicator of skin sensitivity [16]. Compared to baseline, the red area,  $a^*$  and EI significantly increased after single NAFL treatment ( $P<0.05$ ). The EI values continued to increase until the next-day follow-up visit, after which they began to gradually recover. On the control side, skin redness returned to pre-treatment levels after 28 days, when the product side has reached this level within 14 days. Compared to control side, immediate use of the product can indeed quickly reduce erythema (Figure 2a). Compared to baseline, the NAFL combined with product for 28 days showed a significant improvement in skin redness parameters ( $P<0.05$ ). EI values showed this phenomenon earlier (14 days), and at the day 28 follow-up site, the combination of the NAFL and placebo for 28 days also showed significantly improved results ( $P<0.05$ ).

TEWL and hydration are usually involved in determining and measuring barrier function[17]. After NAFL, the levels from both sides showed significant negative changes compared to baseline due to skin barrier damage caused by NAFL. Later, The TEWL continuously decreased from the AF-NAFL at subsequent visits. At the last visit, the TEWL from both sides was significantly decreased compared to baseline, and there was statistical difference between sides. In line with hydration levels, TEWL levels from both groups significantly increased at day 7 compared to baseline, the levels returned towards baseline values at day 14. At all visits, changes of product-treated side were significantly different from the placebo-treated sides. On the other hand, there were significant increments in the hydration from both sides at day 28 compared to baseline (Figure 2b). Skin topography assessments revealed statistically significant improvements in skin roughness, smoothness, scaliness, and wrinkles after 28 days of use the product. Product enhanced the efficacies of 1565-nm NAFL ( $P<0.05$ , comparing to placebo). But the parameter SEsc result on the placebo side showed that skin scaliness increased significantly after the laser until returning to baseline levels after

28 days. The parameter SEsc evaluates the hydration level of stratum corneum; the smaller SEsc is, the greater is the hydration level with less exfoliation. However, skin scaliness was lower on the sample side compared to baseline and the placebo side on the 2th and 4th week. Lower values of skin scaliness showed that the skin got hydrated during the product treatment.

### (2) Skin pigmentation

50% of participants exhibited transient melanin index elevation at one day post-NAFL treatment. MI values began to decline by day 7 post-NAFL, accompanied by improved skin tone as evidenced by ITA enhancement (Table1). While the tested repair product showed no immediate effect on acute melanin elevation, prolonged application (beyond 7 days) demonstrated accelerated melanin clearance. The sequential application of product maintained the good results ( $P<0.05$ , comparing to baseline) and even further decreased the skin MI values ( $P<0.05$ , comparing to placebo). Furthermore, it markedly enhanced skin ITA° values (vs. placebo,  $P<0.05$ ), indicating action in pigment correction.

**Table 1. Skin ITA and MI measurements**

Parameter	Group	BL	Af-NAFL	D1	D7	D14
MI	Product	210.21±36.28	199.88±35.02	208.78±37.81	203.01±37.87	198.28±36.73
	Control	210.24±36.28	199.86±35.08	210.67±37.92	206.61±38.71	203.07±37.34
ITA°	Product	32.32±9.23	38.27±8.55	32.31±7.31	36.33±8.49	36.59±8.53
	Control	32.28±9.15	38.17±8.56	31.72±7.36	35.53±8.56	35.46±8.66

### (3) Skin rejuvenation and collagen density

Employing the VISIA® imaging system for precise measurements, we observed a significant decrease in wrinkle count and size located in the cheek and forehead area. NAFL reduced the fine wrinkles and improved the appearance of the skin. Compared to the control side, the application of the product significantly enhanced this effect ( $P<0.05$ ). Skin elasticity was assessed before and directly after the 1565-nm NAFL, as well as 1, 2, 4 week during product treatment. Compared to baseline, the main parameters R2, R5, R7, R0 and F4 displayed statistically significant improvements on the cheeks after 2 weeks ( $P<0.05$ , Figure 2d). As much, the side that received the product did better than the placebo side. In addition, a significant improvement in pore counts were also detected after NAFL treatment. While enhancing the skin tightening effect, the product also demonstrated a certain degree of efficacy in reducing pores. At baseline, the dermal thickness and collagen density was similar in two sides, and a gradual process of decline and then increase was observed in two sides during 28 days. By day 28, the collagen density on the NAFL combined with placebo side showed significant improvement, while the product side had already achieved similar results by day 7 (Figure 2c,e).

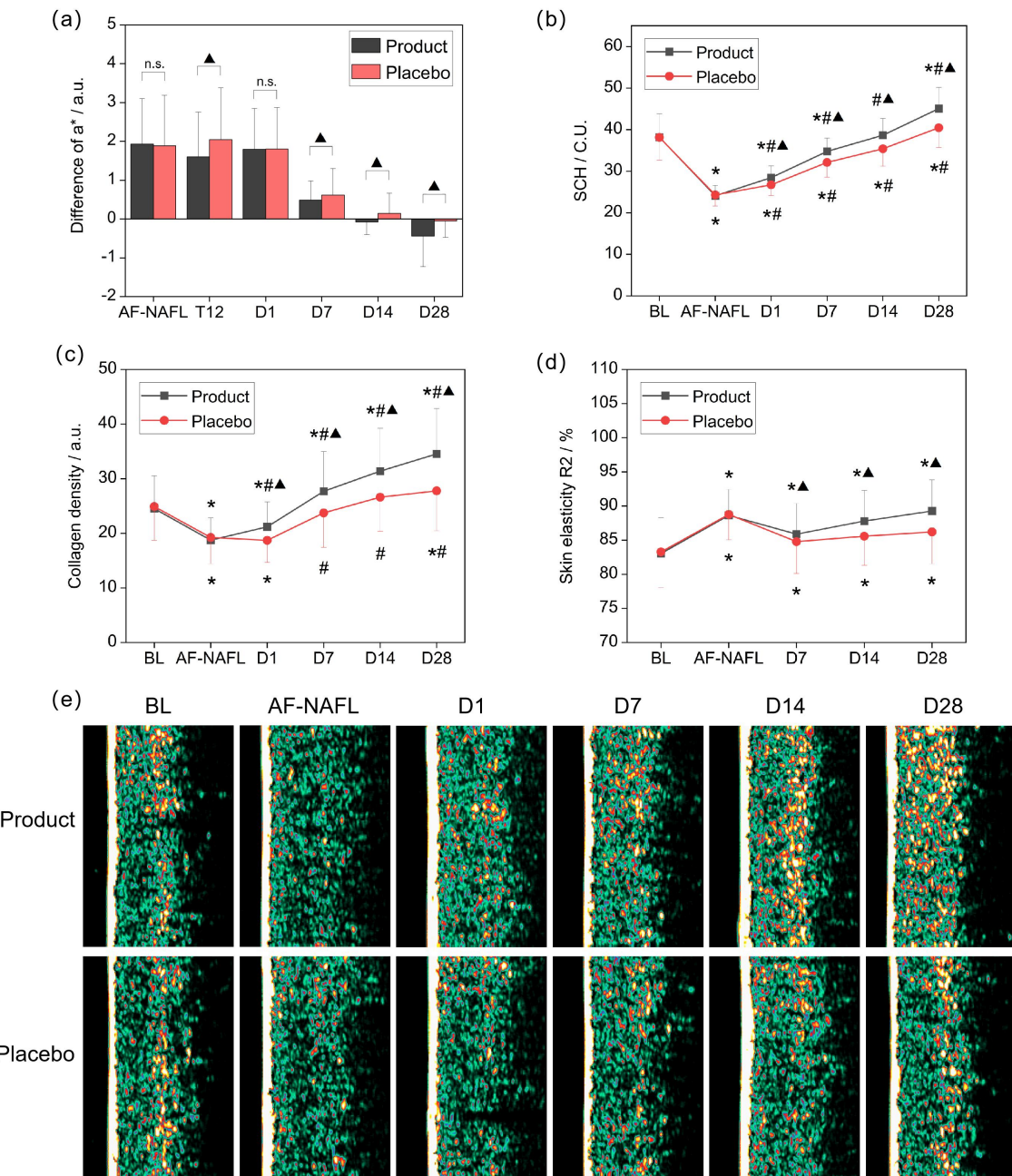


**Figure 2 Differences in skin physiological parameters.** (a) difference of  $a^*$  value (after minus BL); (b) SCH value; (c) collagen density; (d) R2 value; (e) Example Ultrasound photograph from Subject 03.  $p<0.05$  means significant difference, compared with BL, significance was denoted as “\*”, compared with AF-NAFL, significance was denoted as “#”, product vs placebo, significance was denoted as “▲”, “n.s” means no significance.

### 3.3.3 Dermatologist's efficacy assessment and subjects' satisfaction

Comparative clinical evaluation of NAFL therapy paired with the topical product versus NAFL combined with vehicle control demonstrated statistically significant improvements ( $p<0.05$ ) across dermatologist-assessed parameters—including pore, fine line softening, skin brightness, uniformity, and hyperpigmentation attenuation—as well as patient-reported outcomes.

## 4. Discussion

Compared to traditional AFLs, NAFLs based on fractional photothermolysis exhibited fewer adverse effects and shorter recovery periods while improving skin quality[18]. However, the 1565 nm NAFL used in this study may still induce mild secondary reactions, such as edema, erythema, and drying/desquamation (100% incidence). The immediate increase in skin elasticity right after the laser treatment may be related to skin edema. Some of the subjects experienced pruritus, a sense of warmth, tightness, and a tingling sensation. These effects may be associated with the formation of MTZs and the destruction of DEJ caused by NAFL[4]. Additionally, the secondary inflammatory microenvironment maintained skin erythema at a relatively elevated level for up to 24 hours before subsequent decline. Among the Chinese population, while clinically apparent skin adverse reactions resolved within one week, objective instrumental measurements revealed that skin erythema parameters and barrier function indicators (SCH, SEsc, TEWL) required up to 28 days to fully return to preoperative levels. Using the repair products containing rhCOL17 and CERs after the NAFL can exponentially accelerate this process (Day 14 in product vs Day 28 in placebo). Ceramides' established role in skin regeneration through their capacity to restructure lipid matrices and reinforce barrier function[19]. The experimental data from skin damage models demonstrate CERs' dual mechanism of action: suppressing pro-inflammatory cytokines (IL-1 $\alpha$ , PGE2) while upregulating key barrier proteins (FLG, LOR, Keratin 1). The anti-inflammatory properties particularly address post-laser inflammatory responses. The faster resolution of post-NAFL erythema on the product-treated side likely stems from CERs' anti-inflammatory action counteracting laser-induced cytokine surges. At the same time, this created a powerful environment for the skin reconstruction process. Concurrently, rhCol17 exerted its pivotal role by targeted enhancement of DEJ continuity and stimulating structural protein biosynthesis[14]. This study further validated this theory in an ex vivo skin injury model, where TEM imaging demonstrated that topical application of rhCOL17 significantly enhanced the continuity of the DEJ through laminin 5 and collagen IV/VII/XVII upregulation. This effect is anticipated to facilitate the restoration of the basement membrane barrier following laser treatment. This is consistent with the clinical results, where a significant repair effect did occur on the product side.

Notably, although physician assessments revealed no clinically apparent PIH in any subjects, 50% of participants exhibited transient melanin index elevation at one day post-NAFL treatment. This phenomenon may correlate with the large amount of melanin brought out from microscopic epidermal necrotic debris (MENDs) [4], which typically clears within 7 days through natural desquamation. Consequently, MI values began to decline by day 7 post-NAFL, accompanied by improved skin tone as evidenced by ITA enhancement. While the tested repair product showed no immediate effect on acute melanin elevation, prolonged application (beyond 7 days) demonstrated accelerated melanin clearance, potentially mediated through enhanced epidermal turnover and metabolic regulation, thereby amplifying NAFL-mediated skin tone improvement. The precise molecular mechanisms warrant further investigation.

The application of NAFL to achieve skin rejuvenation is based on "destruction-rebuild", such as collagen loss and regeneration[20]. Previous studies showed that NAFL can leads to the loss of type III collagen, the thermally damaged collagen inside the MTZs is completely replaced with new collagen within 3 months[4]. Immunohistochemical analysis demonstrated complete depletion of type III collagen staining within thermally denatured dermal MTZs at 1 hour post-NAFL treatment, followed by progressive intensification of type III collagen immunostaining from day 1 to day 7[4]. This clinical study results demonstrated that collagen density decreased significantly at 30 minutes post-NAFL treatment, reaching its lowest point by day 1. Subsequently, collagen density values began to gradually increase, returning to preoperative levels by day 14 and continuing to rise thereafter. This process was accompanied by improved skin elasticity and reduction in wrinkle severity. The skin care products used in this study also enhanced this function. We validated the dermal collagen I and III remodeling capacity of rhCOL17 using an ex vivo skin model. Notably, the repair product demonstrated unexpectedly high efficacy in restoring post-laser dermal density, with

the product side achieving superior outcomes by day 7 compared to day 14 in the placebo side. The epidermal barrier has long been a critical impediment for active ingredients to penetrate the skin and reach target sites. Multiple studies indicate that laser pretreatment can enhance molecular permeability and penetration depth through controlled barrier ablation[21, 22]. This mechanism would facilitate deeper absorption of rhCOL17 and other bioactive components in the product, thereby maximizing their therapeutic potential. The 1565nm NAFL's fractional photothermolysis creates vertical microchannels, theoretically enhancing rhCOL17 delivery to DEJ and dermal zones. Consequently, this therapeutic synergy imposes more stringent safety requirements on the repair formulations. No subject reported intolerance or allergy to the product during follow-up.

## 5. Conclusion

This clinical study demonstrates the synergistic efficacy and safety profile of combining 1565 nm NAFL with a novel repair essence containing rhCOL17 and CERs for facial rejuvenation. The sequential protocol achieved accelerated recovery from laser-induced inflammation while enhancing long-term improvements in skin texture, pigmentation, and collagen remodeling. The sequential modality of 1565 nm NAFL followed by skincare product was an alternative choice for facial rejuvenation.

## References

- [1]. Wang Yixin, Zhou Chengxia and Li Li, Current status and challenges of skin barrier function repair after photoelectric surgery. *Bulletin of Dermatology*, 2023. 40(06): 656-661.
- [2]. Murray, T.N., J.K. Hu and P.M. Friedman, Full-face and neck resurfacing with a novel ablative fractional 2910 nm erbium-doped fluoride glass fiber laser for advanced photoaging. *Lasers Surg Med*, 2024. 56(3): p. 249-256.
- [3]. Aggarwal, I., et al., Review of Fractional Nonablative Lasers for the Treatment of Dermatologic Conditions in Darker Skin Phototypes. *Dermatol Surg*, 2024. 50(5): p. 459-466.
- [4]. Laubach, H., et al., Skin responses to fractional photothermolysis. *Lasers Surg Med*, 2006. 38(2): p. 142-9.
- [5]. Han, Q., et al., Evaluation of 30% supramolecular salicylic acid followed by 1565-nm non-ablative fractional laser on facial acne and subsequent enlarged pores. *Lasers Med Sci*, 2023. 38(1): p. 91.
- [6]. Kolodziejczak, A. and H. Rotsztejn, Efficacy of fractional laser, radiofrequency and IPL rejuvenation of periorbital region. *Lasers Med Sci*, 2022. 37(2): p. 895-903.
- [7]. Hantash, B.M., et al., Laser-induced transepidermal elimination of dermal content by fractional photothermolysis. *J Biomed Opt*, 2006. 11(4): p. 041115.
- [8]. Su Ming-ying et al., Evaluation of the efficacy of 1565nm nonablative fractional laser on skin. *Journal of Jilin University of Medicine*, 2021. 42(04): 245-247.
- [9]. Liu, X., et al., Comparison of the 1064-nm picosecond laser with fractionated microlens array and 1565-nm non-ablative fractional laser for the treatment of enlarged pores: a randomized, split-face, controlled trial. *Lasers Med Sci*, 2024. 39(1): p. 80.
- [10]. Ng, W.H.S. and S.D. Smith, Laser-Assisted Drug Delivery: A Systematic Review of Safety and Adverse Events. *Pharmaceutics*, 2022. 14(12).
- [11]. Conradt, G., I. Hausser and A. Nystrom, Epidermal or Dermal Collagen VII Is Sufficient for Skin Integrity: Insights to Anchoring Fibril Homeostasis. *J Invest Dermatol*, 2024. 144(6): p. 1301-1310.e7.
- [12]. Sun, W., et al., Comprehensive functional evaluation of a novel collagen for the skin protection in human fibroblasts and keratinocytes. *Biosci Biotechnol Biochem*, 2023. 87(7): p. 724-735.
- [13]. Liu, Y., et al., Targeting the stem cell niche: role of collagen XVII in skin aging and wound repair. *Theranostics*, 2022. 12(15): p. 6446-6454.
- [14]. Wang, J., et al., Recombinant human collagen XVII protects skin basement membrane integrity by inhibiting the MAPK and Wnt signaling pathways. *Mol Med Rep*, 2025. 31(4).

- [15]. Wang, X., et al., Comparison of two kinds of skin imaging analysis software: VISIA((R)) from Canfield and IPP((R)) from Media Cybernetics. *Skin Res Technol*, 2018. 24(3): p. 379-385.
- [16]. Matias, A.R., et al., Skin colour, skin redness and melanin biometric measurements: comparison study between Antera((R)) 3D, Mexameter((R)) and Colorimeter((R)). *Skin Res Technol*, 2015. 21(3): p. 346-62.
- [17]. Pretel-Lara, C., et al., Skin Barrier Function and Microtopography in Patients with Atopic Dermatitis. *J Clin Med*, 2024. 13(19).
- [18]. Schallen, K.P., et al., In Vivo Histological Study Evaluating Non-Ablative Fractional 1940-nm Laser. *Lasers Surg Med*, 2025. 57(1): p. 54-62.
- [19]. Schild, J., et al., The role of ceramides in skin barrier function and the importance of their correct formulation for skincare applications. *Int J Cosmet Sci*, 2024. 46(4): p. 526-543.
- [20]. Zeng, Q., et al., Enhancement of Facial Rejuvenation Through a Combination of 1565 nm Non-Ablative Fractional Laser with 30% Supramolecular Salicylic Acid. *J Vis Exp*, 2024(211).
- [21]. Haghay Khashechi, E., et al., Laser-mediated Solutions: Breaking Barriers in Transdermal Drug Delivery. *AAPS PharmSciTech*, 2024. 25(6): p. 142.
- [22]. Labadie, J.G., et al., Evidence-Based Clinical Practice Guidelines for Laser-Assisted Drug Delivery. *JAMA Dermatol*, 2022. 158(10): p. 1193-1201.